ELSEVIER

Nuclear Physics B (Proc. Suppl.) 69/1-3 (1998) 68-73

NUCLEAR PHYSICS B
PROCEEDINGS
SUPPLEMENTS

RXTE Observations of Cas A

R. E. Rothschild, R. E. Lingenfelter, P. R. Blanco, D. E. Gruber, W. A. Heindl, D. MacDonald, D. F. Marsden, M. R. Pelling, [a] * K. Jahoda, G. E. Allen, J. H. Swank [b] S. E. Woosley [c] K. Nomoto [d] and J. C. Higdon [e]

[a]Center for Astrophysics and Space Sciences, UCSD
9500 Gilman Dr., La Jolla, CA 92093-0424, USA

[b]Code 666, Goddard Space Flight Center
Greenbelt, MD 20771 USA

[c]Board Study Astronomy/Astrophysics, UCSC
Santa Cruz, CA 95064 USA

[d]University of Tokyo, School of Science, Dept. of Astronomy
Bunkyo-ku, 113 Tokyo Japan

[e]The Claremont Colleges, Joint Science Center
11th St & Dartmouth Ave., Claremont, CA 91711 USA

Rossi X-ray Timing Explorer (RXTE) observations of the bright supernova remnant Cas A have revealed a hard power law component above 10 keV in addition to two thermal components inferred from ASCA measurements of the many line centroids from low-Z elements. The power law can be shown to be consistent with synchrotron emission from radio to hard x-rays by electrons of up to 4×10^{13} eV. Measurement of the 1157 keV line by CGRO from ^{44}Sc in the chain of decay of ^{44}Ti predicts that the two ^{44}Ti lines at 68 and 78 keV should appear at the CGRO intensity. RXTE has placed upper limits on such lines that are marginally consistent with the CGRO measurement. Implications of these results on sites for cosmic ray acceleration and nucleosynthesis are discussed.

1. INTRODUCTION

Two of the major questions in astrophysics deal with the acceleration of cosmic rays and the origin and evolution of the chemical elements. While the basic concepts, such as shock acceleration, Fermi mechanisms, the r- and s-processes of nucleosynthesis, are well accepted, detailed verification has been difficult. Both of these questions are intimately related to supernovae and their remnants. Thus, by studying bright supernova remnants, we hope to be able to shed some light on these important aspects of what happens to matter in the Universe.

1.1. Cosmic Ray Acceleration

The observed spectrum of cosmic rays is an $E^{-2.7}$ power law up to $\sim10^{15}$ eV, where it steepens to an $E^{-3.0}$ power law which extends to more than 10^{18} eV. Prevailing wisdom is that galactic cosmic rays are accelerated to $\sim10^{14}$ eV by shocks in supernova remnants, but this has been difficult to confirm observationally. Radio measurements imply acceleration to $\sim10^{10}$ eV, and x-ray measurements of non-thermal power law emission from supernova remnants, such as SN1006 and IC443, have been interpreted as a continuation of the synchrotron emission seen in the radio. These measurements imply the existence of electrons with energies approaching 10^{14} eV, and it is believed that nucleons will also be accelerated to these energies in these environments.

*The HEXTE team acknowledges the support of NASA Contract NAS5-30720

PII S0920-5632(98)00186-8

One can use the synchrotron relation

$$E_\gamma \sim 0.6 B_{\mu G} E_{14}^2 keV \qquad (1)$$

to estimate the maximum electron energies in units of 10^{14} eV, E_{14}, from the maximum detected photon energy in keV, E_γ, and the assumed magnetic field in microGauss, $B_{\mu G}$. Extending the detection of non-thermal emission to higher energies and to more remnants, will aid in our understanding of the fundamental questions of the acceleration sites in the galaxy.

1.2. Explosive Nucleosynthesis

As we learned from Burbidge, Burbidge, Fowler, and Hoyle [1], and from many others, the lighter elements are formed during the nuclear burning process in stars, while the heavier elements are created in supernova explosions. Detection of short-lived isotopes can aid in the understanding of supernovae and refining nucleosynthesis calculations. The details of supernovae light curves and isotopic abundances in grains are affected by these isotopes.

^{44}Ti is produced by explosive Si burning and the freeze out from nuclear statistical equilibrium in supernovae, and is believed to be the primary source of ^{44}Ca [2]. ^{44}Ti decays to ^{44}Sc producing two nuclear lines at 67.9 and 78.4 keV of essentially equal intensity.The ^{44}Sc decays to ^{44}Ca producing a 1.157 MeV photon. All three nuclear lines are expected to have the same line strength. The ^{44}Ti mean life is about 85 years and that for ^{44}Sc is 5.7 years. These three lines can then be used as a signature of young supernovae was well as an indicator of nucleosynthesis.

1.3. Cas A

Cas A is the remnant of the explosion of a massive star about 300 years ago at a distance of ~3 kpc. If indeed Flamsteed observed it in 1680, its age is 317 years and it was markedly dim for a massive star. Optical observations suggest the progenitor was greater than 25 $M_\odot$ — most probably a Wolf-Rayet star, and that the supernova was a type Ib or type II. X-ray imaging of Cas A has revealed an outer, weak ring of emission that is assumed to be the expanding shock wave interacting with the interstellar medium or the wind from the progenitor. There is also a brighter inner ring representing the reverse shock impinging on the ejecta.

Measurements by ASCA [3] have shown that thermal equilibrium has not been reached and that simple one- or two-temperature thermal models are insufficient to model the data. Measurements above 10 keV by HEAO-1, CGRO, and other high energy missions require a non-thermal component must also be present. The presence of 13 line features in the ASCA spectrum tells us that at least two temperatures are present — one for the non-Fe elements and one for Fe itself.

The COMPTEL on CGRO has discovered and mapped the 1.157 MeV nuclear line from ^{44}Sc decay coming from Cas A [4].The COMPTEL map clearly shows the line radiation coincident with the position of Cas A. The spectrum shows the significant measurement of the line and the nearby energy bins. According to COMPTEL calculations, about 1×10^{-4} $M_\odot$ of ^{44}Ti is inferred to have been produced. This large amount of ^{44}Ti is consistent with some models by Woosley and co-workers, Nomoto, and Thielemann, but it predicts a much brighter supernova than apparently occured.

The OSSE instrument on CGRO has also made observations of Cas A in the 40 keV to few MeV range, and does not detect either the 1.157 MeV line or the two hard x-ray lines in the 70–80 keV range [5]. The OSSE 99% upper limit of 5.7×10^{-5} $\gamma/cm^2 s$ is still consistent with the COMPTEL value of $(4.2\pm0.9)\times 10^{-5}$ γ/cm^2 s. OSSE observed the continuum to ~100 keV to be a power law with photon index $3.06^{+0.41}_{-0.44}$.

2. RXTE OBSERVATIONS

Cas A has been viewed 4 times during the RXTE mission: 2 long 200 ks observations in AO-1 and AO-2, once in IOC, and once as a calibration observation. Results from the two long observations will be presented.

2.1. Instrumentation

The observations were made with both the Proportional Counter Array (PCA) [6] and the High Energy X-ray Timing Experiment (HEXTE) [7].

These instruments are coaligned with the same 1° FWHM field of view and together they cover the 2–250 keV range. The line search and extension of the non-thermal flux maximum energy to high energies is mostly in the perview of the HEXTE instrument, so I shall describe it in more detail.

The HEXTE is comprised of 8 NaI/CsI phoswich scintillation detectors of 200 cm^2 each and grouped 4 to a cluster. Each detector's field of view is limited by a lead collimator to 1° FWHM, and the gain of each detector system is actively controlled. The ^{241}Am calibration and gain control centroid is stable to 0.02 PHA channels on a one-day timescale. One PHA channel is approximately 1 keV in width. The entire detector-collimator-anticoincidence shield assembly is rocked on- and off-source with 16 s dwell times at each position. The rotation axes of the two clusters are orthogonal to each other, enabling 4 background regions to be sampled around a given source.

2.2. HEXTE Background

Of primary importance to this investigation is the background subtraction afforded by the rocking of the HEXTE clusters. HEXTE background subtraction performance is clear in the following examples. First of all, during In-Orbit Checkout (IOC), RXTE viewed 19 blank fields all over the sky for 10 minutes each. Figure 1 shows the net counting rate (i.e., on-source minus the sum of the two off-source observations) in four energy bands for the 19 observations. The energy bands are 16-30, 31-60, 61-100, and 101-240 keV. The crosses are cluster A and the boxes are cluster B. The dotted lines represent zero net flux, and as you can see, these short observations are consistent with no blank sky net flux.

Secondly, we have the net spectrum of the difference of the two off-source positions for a 200 ks observation of MCG 8-11-11 during the IOC period (Figure 2). The data are binned every 5 PHA channels (~5 keV) over the entire 15-250 keV HEXTE energy range. The twin dashed lines represent ±1% of background and the rates are expressed as percent of background. Clearly, any systematics in background subtraction are of order less than 1% of background.

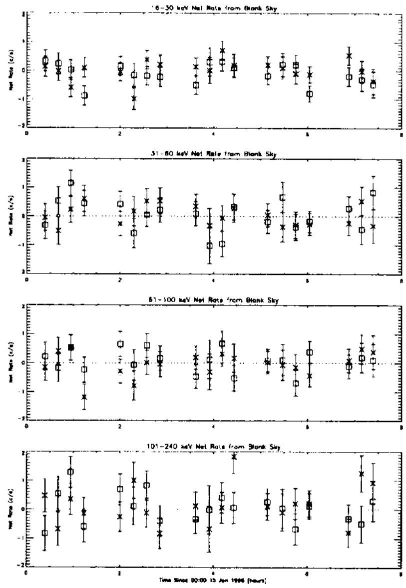

Figure 1. Background subtracted counting rates for 19 ten-minute observations of blank fields on 15 January 1996. The four sets of rates cover the energy range 16-30, 31-60, 61-100, and 101-240 keV. The crosses (x) represent Cluster A and boxes (□) Cluster B. The dotted line indicates zero net flux.

Finally, as part of an investigation of the spectrum of the diffuse flux fluctuations, we were awarded the off-source data for all observations greater than 50 ks. We have separately accumulated the two off-source spectral histograms for observations with a range of orbital and environmental parameters. Figure 3 displays the net off-source spectrum along with lines to denote ±0.5% of background for 5×10^6 s. Again, the systematics are less than 0.5% of background.

3. RESULTS

We present results on the two long 200 ks observations made in AO-1 and AO-2. All spectral analyses were made using XSPEC 10.0, after extracting the PCA data with the Guest Observer

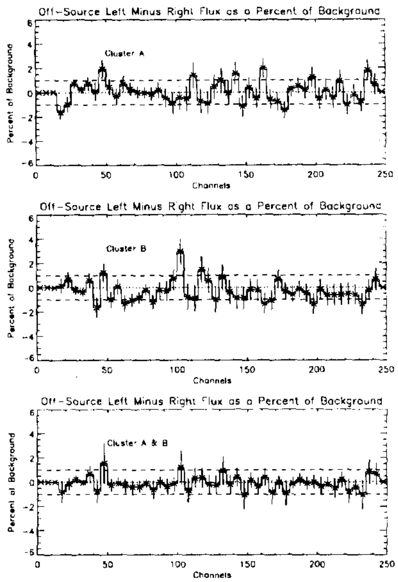

Figure 2. The net counting rate histogram of the difference of the two off-source positions for each cluster and their sum during the MCG 8-11-11 observation. One percent of the total off-source flux is shown by pairs of horizontal dashed lines for comparison. "Left" and "Right" correspond to the plus and minus directions of the off-source viewing.

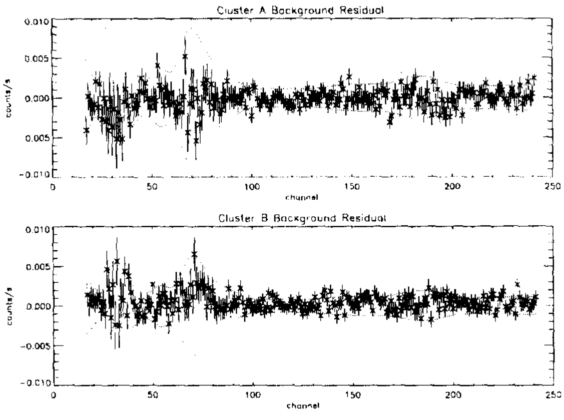

Figure 3. The net off-source counting rate histogram versus pulse height channel for a 5×10^6 s accumulation of observations with greater than 50 ks duration for the two HEXTE clusters. The detector gain is approximately one keV per channel, and the energy range covered is 15−240 keV. The dotted lines represent $\pm0.5\%$ of the background per channel.

Facility supplied ftools and the HEXTE data with UCSD specific IDL software.

3.1. Continuum

RXTE clearly sees the E^{-3} power law continuum, as seen by ASCA and other missions, above 10 keV. Below this energy, the continuum is a combination of the power law and the thermal bremsstrahlung associated with the line emission. The iron K line is clearly seen, also. This work has been reported by Allen et al. [8]. One can estimate the temperatures of the various thermal distributions necessary to produce the observed lines in the ASCA data. Two are required: 1) kT=0.7 keV will reproduce the light elements (Ne, Mg, Si, S, Ar, and Ca), and 2) kT=2.8 keV for the Fe line. As seen before, a power law dominates these thermals above 10 keV with an index of about 3. Such a power law cannot continue well below 10 keV, or it will be in conflict with the thermal components. Indeed, fitting the ASCA data with just a power law for the continuum gives an acceptable fit [3]. This indicates the high energy power law must flatten at these energies.

We fit the ASCA GIS and the RXTE PCA/HEXTE data simultaneously with a model containing 2 Raymond-Smith thermals, a broken power law, and a gaussian at 6.4 keV to represent iron on grains in Cas A. The best fit for the broken power law had a low energy index of 1.8 that broke at 16 keV to 3. If we represented the high energy flux with another thermal, a significantly worse fit was achieved for kT=24 keV.

Various possible origins of the power law flux have been discussed [8], with the conclusion that, since pulsed flux is not detected in the range of 1 ms to 10 s, synchrotron emission is most likely. Assuming this origin and assuming a 1 mG equipartition magnetic field, we find the maximum electron energy to be at least 4×10^{13} eV. If accelerated electrons exist at these energies, protons are also expected to experience the same acceleration for energies much larger than the rest mass of the proton [9]. Thus, if Cas A is typical, supernova remnants can provide the acceleration for cosmic rays at least to these energies.

3.2. ^{44}Ti Lines

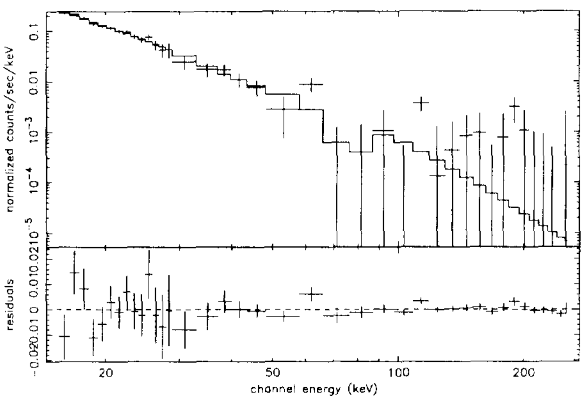

Figure 4. HEXTE counts histogram plus model fit for the AO-1 observation of Cas A. The lower panel displays the residuals to the model fit.

We searched the two long observations of Cas A for the ^{44}Ti lines at 68 and 78 keV, and the two observing periods gave very different results. As I have demonstrated, the HEXTE background subtraction has systematic uncertainties at less than 0.5% of background. Yet, in AO-1, there is evidence of an oversubtraction of background at the 1-2% level. Since the lead collimator produces fluorescence lines at 74 and 85 keV, and an iodine activation line is present at 66 keV, this oversubtraction greatly affects the search for the ^{44}Ti lines. Figure 4 shows the best fit of the AO-1 HEXTE data to a power law plus two gaussians model. The line energies were

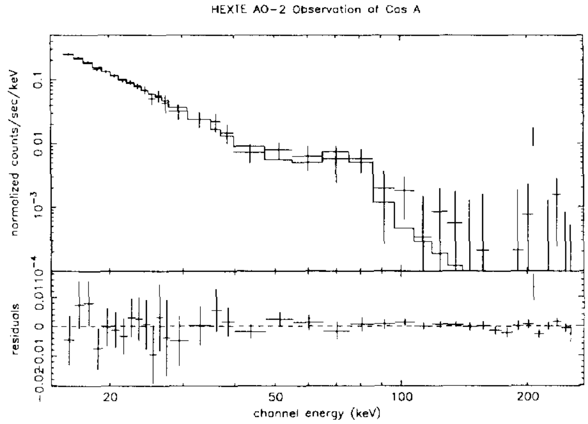

Figure 5. HEXTE counts histogram plus model fit for the AO-2 observation of Cas A. The lower panel displays the residuals to the model fit.

fixed at the known ^{44}Ti values and the widths of the lines were broadened by 2.5% to account for the expansion velocity of Cas A, assuming a nominal value of 7500 km/s [10]. The value for the flux of both lines is $(-1.4\pm1.7)\times10^{-5}$ γ/cm^2 s for both clusters fit simultaneously. The power law is 3.09 ± 0.10 with a 20-50 keV flux of $(3.2\pm0.2)\times10^{-11}$ ergs/cm^2 s.

The other long observation, fit similarly, yields evidence for excess emission at 68 and 78 keV, as shown in Figure 5. The best fit line flux was $(4.3\pm1.8)\times10^{-5}$ γ/cm^2 s, which is in excellent agreement with the COMPTEL result. Until, however, the discrepancy between the two observations is resolved, I cannot claim a true detection. If we combine the two data sets and fit them, the result for the line flux is $(1.3\pm1.2)\times10^{-5}$ γ/cm^2 s, or a 90% upper limit of 3.3×10^{-5} γ/cm^2 s.

4. CONCLUSIONS

The PCA/HEXTE instruments on RXTE have detected x-ray emission from Cas A in the range 2-100 keV. The continuum above 10 keV is a power law with photon index ~3, which we have interpreted as due to synchrotron processes within the remnant. No pulsations are detected in the 1 ms to 10 s range. Assuming an equipartition magnetic field of 1 mG, we infer that electrons are accelerated up to at least 4×10^{13} eV. Previous theoretical work has demonstrated that nucleons will also be accelerated to the same energies, and thus, supernova remnants are capable of providing the acceleration mechanism for cosmic rays in the galaxy, at least to $\sim10^{14}$ eV.

The search for hard x-rays from ^{44}Ti decay at 68 and 78 keV had mixed results. One observation agreed with the COMPTEL measurement of the 1.157 MeV line and one did not detect any line flux at all. This latter measurement is suspect due to the clear indication of an oversubtraction of background. Until this discrepancy is resolved, no definitive statement can be made.

REFERENCES

1. E.M. Burbidge, G.R. Burbidge, W.A. Fowler, & F. Hoyle 1957, RMP, 29, 547.
2. F.X. Timmes, S.E. Woosley, D.H. Hartmann, & R.D. Hoffman 1996, ApJ, 464, 332.
3. S.S. Holt, E.V. Gotthelf, H. Tsunemi, & H. Negoro 1994, PASJ, 46, L151.
4. A.F. Iyudin et al. 1994, A&A, 284, L1.
5. L.-S. The et al., A&ASS 1996, 120, 357.
6. K. Jahoda et al. 1996, in EUV, X-ray and Gamma-ray Instrumentation for Space Astronomy VII, ed. O.H.W. Siegmund & M.A. Grummin, Proc. SPIE 2808, 59.
7. R.E. Rothschild et al. 1998, ApJ, in press.
8. G.E. Allen et al. 1997, ApJ, in press.
9. D.C. Ellison & S.P. Reynolds 1991, ApJ, 382, 242.
10. R.A. Fesen, R.H. Becker, & R.W. Goodrich 1988, ApJ, 329, L89.